A 3-D Polynomial-Chaos FDTD Technique for Complex Inhomogeneous Media with Arbitrary Stochastically-Varying Index Gradients

Georgios G. Pyrialakos [1], Theodoros T. Zygiridis [2], and Nikolaos V. Kantartzis [1]

[1] Department of Electrical and Computer Engineering
Aristotle University of Thessaloniki, Thessaloniki, 54124, Greece
pyrialak@auth.gr, kant@auth.gr

[2] Department of Informatics and Telecommunications Engineering
University of Western Macedonia, Kozani, 50100, Greece
tzygiridis@uowm.gr

Abstract ─ An enhanced finite-difference time-domain algorithm featuring the polynomial chaos representation is introduced in this paper for problems with stochastic uncertainties. Focusing on the solution of the governing partial differential equations, the new 3-D method uses the Karhunen-Loève expansion to effectively decorrelate random input parameters denoted by stochastic processes. So, the space dimension is seriously reduced and high accuracy levels are attained, even for media with abrupt and fully unknown statistical variations. These profits are verified via a detailed numerical study.

Index Terms ─ Advanced FDTD methods, polynomial chaos, random media, stochastic process, uncertainties.

I. INTRODUCTION

The assessment of stochastic uncertainties, inherent in electromagnetics, has been of pivotal significance, so leading to different numerical schemes. Amid them the Monte Carlo (MC) approach [1], albeit accurate, has proven time-consuming, due to its excessively many realizations and slow convergence to the desired result. Recently, efficient techniques have been presented [2-6], such as the generalized polynomial chaos finite-difference time-domain (GPC-FDTD) algorithm [7, 8]. Usually, uncertainties emerge from discrete stochastic variables or processes that vary in an unknown way. Being difficult to model, the latter cannot be directly plugged in the GPC-FDTD technique, as they require an infinite number of correlated random variables.

To overcome such an issue, this paper develops a 3-D GPC-FDTD methodology for complex materials with arbitrary statistically-varying index gradients. The novel algorithm utilizes an orthogonal field expansion over the space of random parameters, so minimizing the error for both the mean value and variance. While it is primarily optimized for the extraction of the first two moments, the approximated relation between the output and stochastic parameter can provide with more valuable information like the computation of high-order statistical moments or maxima/minima, useful in electromagnetic compatibility (EMC) applications [9, 10]. To decrease the dimension of space spanned by the input parameters and decorrelate them, the Karhunen-Loève scheme is employed. It transforms the infinite product space of random inputs to be described by a new base that can be safely truncated. The resulting variables are, also, uncorrelated, which for Gaussian processes is equivalent to independence; an ample claim for the GPC applicability. Numerical outcomes certify our method, accelerated via graphics processor units (GPUs), and reveal its superiority.

II. PROPOSED METHODOLOGY

A. Generalized polynomial chaos expansion

The GPC method expands all fields in a summation of orthogonal, under an inner product, basis functions over space $\Omega = \cup\Omega_i$ (i = 1,2,…,D), spanned by all D random variables ω_i (each defined in Ω_i), on condition that they are statistically independent. The orthogonality is satisfied with respect to the inner product:

$$\begin{aligned}\left\langle \Theta_a(\boldsymbol{\omega}), \Theta_b(\boldsymbol{\omega}) \right\rangle &\triangleq \int_{\Omega} \Theta_a(\boldsymbol{\omega}) \Theta_b(\boldsymbol{\omega}) w(\boldsymbol{\omega}) d\boldsymbol{\omega} \\ &= \left\langle \Theta_a(\boldsymbol{\omega}), \Theta_a(\boldsymbol{\omega}) \right\rangle \delta_{a,b},\end{aligned} \tag{1}$$

with $\Theta_{a,b}(\boldsymbol{\omega})$ the basis functions, $\boldsymbol{\omega} = [\omega_1,\omega_2,\ldots,\omega_D]^{\mathrm{T}}$ the vector formed by ω_i, $\delta_{a,b}$ the Kronecker's delta, and $w(\boldsymbol{\omega})$ the distribution function of $\boldsymbol{\omega}$. Note that, in the case of a single random variable ω_i, the most common $w(\omega_i)$ are related to well-known polynomials like the Hermite (Gaussian distribution), the Jacobi (beta distribution), and the Legendre (uniform distribution) polynomials. However, in the multivariate case, $\Theta_{a,b}(\boldsymbol{\omega})$ are generally unknown, unless a statistical independence between the random variables is guaranteed [8]. Only then $\Theta_{a,b}(\boldsymbol{\omega})$ may be expressed as the product of the prior polynomials related to their known distributions, i.e.,

Submitted On: December 31, 2015
Accepted On: April 26, 2016

$$\Theta_a(\boldsymbol{\omega}) = \prod_{i=1}^{D} \Theta_{a_i}(\omega_i), \tag{2}$$

where $\Theta_{ai}(\omega_i)$ is a univariate basis in ω_i of polynomial order a_i. So, any electric/magnetic component $F = \{E_x, E_y, E_z, H_x, H_y, H_z\}$ in the FDTD domain is written as:

$$F\big|_{i,j,k}^{n}(\boldsymbol{\omega}) = \sum_{a=0}^{P} f^a\big|_{i,j,k}^{n} \Theta_a(\boldsymbol{\omega}), \tag{3}$$

with f^a the corresponding coefficients and P the number of polynomials, calculated for the highest order N, by:

$$P = \binom{N+D}{N} = \frac{(D+N)!}{D!N!}. \tag{4}$$

Note that the GPC technique can not directly treat cases, where stochastic processes affect the output, since the latter are described by an infinite series of correlated random variables indexed by some physical coordinate. In contrast, the FDTD discretization can hardly offer any benefit, since one ends up with a very large (although not infinite) number of correlated random variables.

B. Karhunen-Loève stochastic representation

To overcome these issues, we launch the Karhunen-Loève (KL) expansion [8] for both the dimension reduction and decorrelation of the stochastic processes. Let $Y_x(\boldsymbol{\omega})$ be a stochastic process varying over coordinate $x \in [p, q]$ bounded domain, with a covariance function of $C(x_1, x_2)$. The KL expansion of $Y_x(\boldsymbol{\omega})$ reads:

$$Y_x(\boldsymbol{\omega}) = m\{Y_x(\boldsymbol{\omega})\} + \sum_{i=0}^{\infty} \sqrt{\lambda_i}\, \psi_i(x) Y_i(\boldsymbol{\omega}), \tag{5}$$

where $m\{Y_x(\boldsymbol{\omega})\}$ is the mean value of $Y_x(\boldsymbol{\omega})$ and $Y_i(\boldsymbol{\omega})$ are centered, uncorrelated random variables of unit variance. Eigenfunctions $\psi_i(x)$ and their respective eigenvalues λ_i are determined via the eigenvalue problem:

$$\int_{[p,q]} C(x,l)\psi_i(l)\, dl = \lambda_i \psi_i(x). \tag{6}$$

Note that for Gaussian processes, $Y_i(\boldsymbol{\omega})$ are generated as independent random variables. Also, when the process is stationary, i.e., its covariance can be written as $C(x_1, x_2) = C(x_2 - x_1)$, the solution of (6) is equivalent to the Fourier transform of $C(x)$, assuming it is periodic outside $[p, q]$. A key trait of the KL expansion (and a motive for its choice in our method) is the decay of λ_i as i increases. So, it is possible to describe the entire stochastic process with only a small truncated series of $Y_i(\boldsymbol{\omega})$.

C. Enhanced GPC-FDTD update equations

The update equations of the 3-D algorithm are extracted by plugging (3) into the leapfrog formulas [9]. The stochastic process (randomness source) $Y_x(\boldsymbol{\omega})$, in the KL expansion (5), is the relative electric permittivity $\varepsilon_r(\boldsymbol{\omega})$, where x can be any coordinate. By replacing $Y_i(\boldsymbol{\omega})$ with ω_i in (5), defining Ω, and truncating the infinite sum up to a K (KL truncation limit), we get:

$$M = m\{\varepsilon_r(\boldsymbol{\omega})\}\varepsilon_0 + \sum_{i=0}^{K} \sqrt{\lambda_i}\, \psi_i(x)\omega_i, \tag{7}$$

which is a very accurate approximation. For instance, the E_z coefficients are given by:

$$\begin{aligned}\sum_{a=0}^{P} e_z^a\big|_{i,j,k+1/2}^{n+1} \Theta_a(\boldsymbol{\omega}) &= R_1 \sum_{a=0}^{P} e_z^a\big|_{i,j,k+1/2}^{n} \Theta_a(\boldsymbol{\omega}) \\ &+ R_2 \left[\begin{array}{l} \frac{1}{\Delta x} \sum_{a=0}^{P} \left(h_y^a\big|_{i+1/2,j,k+1/2}^{n+1/2} - h_y^a\big|_{i-1/2,j,k+1/2}^{n+1/2} \right) \Theta_a(\boldsymbol{\omega}) \\ -\frac{1}{\Delta y} \sum_{a=0}^{P} \left(h_x^a\big|_{i,j+1/2,k+1/2}^{n+1/2} - h_x^a\big|_{i,j-1/2,k+1/2}^{n+1/2} \right) \Theta_a(\boldsymbol{\omega}) \end{array} \right],\end{aligned} \tag{8}$$

with $R_1 = (2M - \sigma'\Delta t)/(2M + \sigma'\Delta t)$, $R_2 = 2\Delta t/(2M + \sigma'\Delta t)$, and σ' the losses. Due to (3), only the respective e^a coefficients are involved. To derive the update equation for every a, we use a Galerkin process, which takes the inner product, as in (1), on both sides of (8) with the respective basis function. Thus, one arrives at:

$$\begin{aligned} e_z^a\big|_{i,j,k+1/2}^{n+1} &= \frac{1}{\theta} \sum_{b=0}^{P} e_z^b\big|_{i,j,k+1/2}^{n} \left\langle R_1 \Theta_a(\boldsymbol{\omega}), \Theta_b(\boldsymbol{\omega}) \right\rangle \\ &+ \frac{1}{\theta} \sum_{b=0}^{P} \left[\begin{array}{l} \frac{1}{\Delta x} \left(h_y^b\big|_{i+1/2,j,k+1/2}^{n+1/2} - h_y^b\big|_{i-1/2,j,k+1/2}^{n+1/2} \right) \\ -\frac{1}{\Delta y} \left(h_x^b\big|_{i,j+1/2,k+1/2}^{n+1/2} - h_x^b\big|_{i,j-1/2,k+1/2}^{n+1/2} \right) \end{array} \right], \\ &\cdot \left\langle R_2 \Theta_a(\boldsymbol{\omega}), \Theta_b(\boldsymbol{\omega}) \right\rangle \end{aligned} \tag{9}$$

for $\theta = \langle \Theta_a(\boldsymbol{\omega}), \Theta_a(\boldsymbol{\omega}) \rangle$, while similar expressions hold for the other components. Note that the stability of the algorithm is specified by the usual Courant condition, which yields flexible time-steps and is proven remarkably efficient (also stated in [7]), as no late-time instabilities were observed in any of our simulations. Consequently and along with the scheme's enhanced dispersion behavior, cases with challenging variations are precisely handled.

All inner products in (9) hold only in the region with the random medium and reduce to $\delta_{a,b}$ elsewhere. Their evaluation is conducted (prior the FDTD update) for each coordinate in the region and is trivial for up to second order of the KL limit K. For higher-order approximations, (1) may be split into 1-D integrals, on condition that (2) holds. Therefore, via a Taylor series expansion of ω_i in every inner product of (9), for an arbitrarily large order s_i (even up to 10 is viewed trivial), we compute:

$$I_{s_i}^{a_i,b_i} = \int_{\Omega_i} \omega_i^{s_i} \Theta_{a_i}(\omega_i)\, \Theta_{b_i}(\omega_i)\, w(\omega_i)\, d\omega_i \ , \tag{10}$$

only once, and apply the Taylor expansion. For example, the second inner product in (9) is expressed as:

$$\left\langle R_2 \Theta_a(\boldsymbol{\omega}), \Theta_b(\boldsymbol{\omega}) \right\rangle = \sum_{s_1}^{D_T} \sum_{s_2}^{D_T} \cdots \sum_{s_K}^{D_T} T_{s_1, s_2, \ldots, s_K} \prod_{d=1}^{D} I_{s_d}^{a_d, b_d}, \tag{11}$$

with T_s the respective Taylor coefficients and D_T the maximum Taylor series order. As a consequence, extra accuracy can be consistently accomplished.

III. GPU/CUDA IMPLEMENTATION

For its acceleration, the 3-D algorithm is parallelized for GPUs via the CUDA platform [11, 12], where different code parts are optimized for enhanced thread concurrency. As the coalescing mechanism is critical, all GPC coefficient matrices are accessed throughout the kernel code. Also, read-only matrices in each kernel are accessed through the texture buffer to increase performance. Then, the shared memory is used to load the pre-calculated inner products for all threads related to spatial coordinates that exhibit material stochasticity. For the 3-D convolution perfectly matched layers (CPMLs) [9], diverse kernels are initialized for each side and field component, executed concurrently by different streams. Hence, the proper grid and block alignment for every kernel is separately fulfilled. To evade errors at mesh corners, we use advanced atomic operators [6]. The acceleration of GPU codes compared to their conventional CPU (serialized) realizations, exceeds the promising value of 50 times.

IV. NUMERICAL RESULTS

The new technique is validated via 3-D setups terminated by 8-cell CPMLs. We examine a *z*-directed wire current source that illuminates an infinite planar dielectric surface at the $y = 0$ plane, featuring a non-uniform (toward *x* direction) stochastic permittivity (Fig. 1 (a)). The distribution function follows the Gaussian norm, hence Hermite polynomials are used as the basis functions. Also, the statistical moments of a domain point occupied by the random medium are $m\{\varepsilon_r\} = 3$ for the mean value and $\sigma\{\varepsilon_r\} = 0.02\ m\{\varepsilon_r\}$ for the standard deviation. Our correlation function is defined as $C(x - t) = e^{-(|x-t|/\alpha)}$, with α the correlation length, while higher *a* translate to larger variations between neighboring points. The problem is divided into 317×317×317 cells, whose size is fixed and equal to the one tenth of the wavelength corresponding to the central frequency of the Gaussian excitation pulse. Also, the time increment is set at the level of 100-150 psec via the Courant condition, while the MC-FDTD scheme gives the reference solution. It generates 5000 different stochastic processes for the dielectric scattering surface. The determined confidence intervals, considered from a 10000 realization reference, do not exceed the 10% and 1% mark for 1000 and 5000 simulations respectively. Any choice beyond this level results in a marginal improvement. Figure 1 (a) depicts three stochastic processes for $\alpha = 0.5$ and Fig. 1 (b) shows the first five eigenfunctions $\psi_i(x)$ produced by the eigenvalue problem (6). The weighted addition of the infinite series of polynomials gives exactly the spatial variation of the dielectric slab. Thus, a higher *K* order, including up to the *K*th eigenfunction, accounts for larger spatial variations. As these play a decreasingly serious role due to the nature of the electromagnetic wave solution the truncation is safely justified.

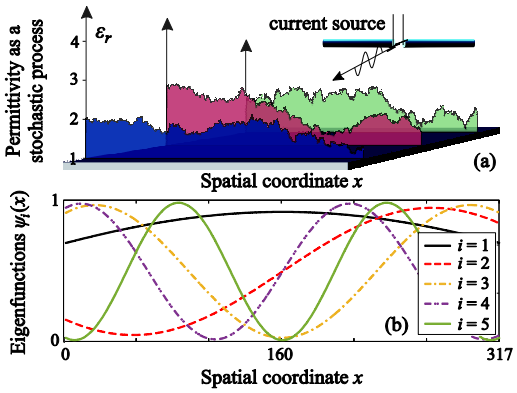

Fig. 1. (a) Perspective 3-D view of the simulation setup with the randomly generated stochastic processes, and (b) eigenfunctions $\psi_i(x)$ for $C(x - t) = e^{-(|x-t|/\alpha)}$ and $\alpha = 0.5$.

We, next, solve the problem for a KL limit up to $K = 3$ ($\alpha = 0.5$, $N = 3$). The choice of *N* is justified as the best compromise between accuracy and computational efficiency. Also, for larger *K* the system burden does not seem to justify the poor increase in accuracy. Figure 2 gives the electric field variance, where the plotted curves are snapshotted at a time-step near the peak of the Gaussian pulse, along the white line of the inlet figure. A clear improvement is attained as *K* augments, yet the difference between the $K = 2$ and 3 curve is very small.

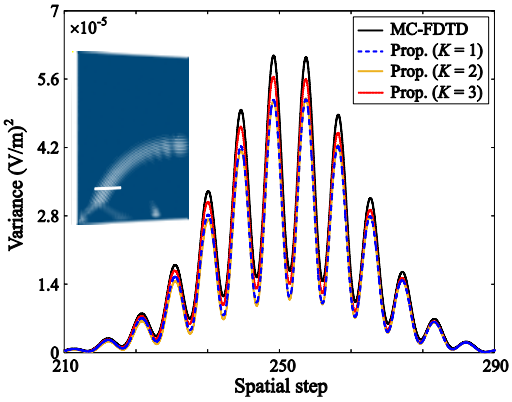

Fig. 2. Electric field variance via 5000 MC-FDTD runs and the proposed method for $\alpha = 0.5$ and $N = 3$.

Finally, Fig. 3 presents the variance of the electric field for $\alpha = 0.5$, yet with a prefixed $K = 4$ and a variety of GPC orders *N*. Apparently, convergence is slower in this case, revealing that the KL truncation limit has a more substantial impact compared to that of *N*. In contrast, it seems that the opposite situation holds for higher correlation length values of the random medium dielectric permittivity, where it is better to optimize *N* in an effort to accomplish the desired approximation.

The main benefit of our algorithm is that via the GPC-KL formulation, one gets a similar approximation

order as with the MC-FDTD approach. While the latter requires thousands of FDTD solutions, the complexity of the former (analogous to *P*) is lower by two magnitude orders. Thus, we can reach a sufficient convergence by analyzing simulations with ascending *K* and *L* orders and keep the efficiency over an exact MC study. It is true, however, that memory can be up to two or even five to ten times higher, in relation with *K* and *L*. So, when memory is not an issue, the GPC-KL method is a powerful alternative. The GPU/CUDA implementation, while it does not add to the theoretical analysis, it is essential for the results assessment in rational times and so it is fully preferred over CPU for both methods.

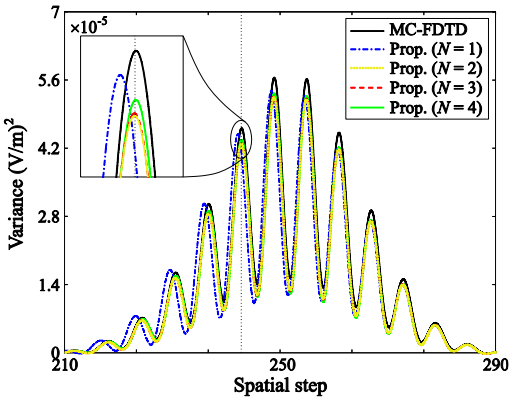

Fig. 3. Electric field variance via 5000 MC-FDTD runs and the proposed method for $\alpha = 0.5$ and $K = 4$.

V. CONCLUSION

The rigorous modeling of inhomogeneous materials with complex statistical index gradients, is presented in this paper via a consistent 3-D GPC-FDTD method. The 3-D technique utilizes the efficient Karhunen-Loève expansion to handle the arbitrary stochastic processes. Results prove the profits of the proposed concept.

REFERENCES

[1] F. Hastings, J. Schneider, and S. Broschat, "A Monte Carlo FDTD technique for rough surface scattering," *IEEE Trans. Antennas Propag.*, vol. 43, no. 11, pp. 1183-1191, Nov. 1995.

[2] M. Wong, J. Carette, A. Hadjem, and J. Wiart, "Stochastic electromagnetic modeling with uncertain dielectric properties using FDTD," in *Proc. 24th ACES Conf.*, pp. 450-455, 2008.

[3] M. Gilbert and F. Teixeira, "A small-perturbation automatic-differentiation method for uncertainty in electromagnetics," *IEEE Trans. Antennas Propag.*, vol. 60, no. 11, pp. 5305-5314, Nov. 2012.

[4] T. Tan, A. Taflove, and V. Backman, "Single realization stochastic FDTD for weak scattering waves in biological random media," *IEEE Trans. Antennas Propag.*, vol. 61, no. 2, pp. 818-828, 2013.

[5] B. T. Nguyen, C. Furse, and J. J. Simpson, "A 3-D stochastic FDTD model electromagnetic propagation in ionosphere plasma," *IEEE Trans. Antennas Propag.*, vol. 63, no. 1, pp. 304-313, 2015.

[6] G. Pyrialakos, T. Zygiridis, N. Kantartzis, and T. Tsiboukis, "GPU-based calculation of lightning-generated fields in 3D problems with statistically defined uncertainties," *IEEE Trans. Electromagn. Compat.*, vol. 57, no. 6, pp. 1556-1567, Dec. 2015.

[7] A. Austin and C. Sarris, "Efficient analysis of geometrical uncertainty in the FDTD ethod using PC for microwave circuits," *IEEE Trans. Microw. Theory Tech.*, vol. 61, no. 12, pp. 4293-4301, 2012.

[8] D. Xiu and G. Karniadakis, "The Wiener-Askey polynomial chaos for stochastic equations," *SIAM J. Sci. Comput.*, vol. 24, no. 2, pp. 619-644, 2002.

[9] A. Taflove and S. C. Hagness, *Computational Electrodynamics: The Finite-Difference Time-Domain Method*. Artech House, Boston, MA, 2005.

[10] H. W. Ott, *Electromagnetic Compatibility Engineering*. Wiley, New York, NY, 2009.

[11] V. Demir and A. Z. Elsherbeni, "Compute unified device architecture (CUDA) based finite-difference time-domain (FDTD) implementation," *ACES J.*, vol. 25, no. 4, pp. 303-314, Apr. 2010.

[12] A. Capozzoli, C. Curcio, G. D'Elia, A. Liseno, and P. Vinetti, "Fast CPU/GPU pattern evaluation of irregular arrays," *ACES J.*, vol. 2, pp. 355-272, 2010.